Hierarchical SAPO-34 preparation based on the crystal metastability in mother liquor solution

Ji Han, Guoju Yang, Yongcun Zou, Xiaoxin Chen, Valentin Valtchev

Hierarchical SAPO-34 preparation based on the crystal metastability in mother liquor solution

Ji Han, Guoju Yang, Yongcun Zou, Xiaoxin Chen and Valentin Valtchev*

J. Han, Dr. G. Yang, Y. Zou, Dr. X. Chen
State Key Laboratory of Inorganic Synthesis & Preparative Chemistry, College of Chemistry, Jilin University, 2699 Qianjin Street, Changchun 130012, P. R. China.
E-mail: chenxiaoxin@jlu.edu.cn

Dr. G. Yang
International Centre of Future Science, Jilin University, 2699 Qianjin Street, Changchun 130012, P. R. China.

Dr. V. Valtchev[1,2]
[1] Qingdao Institute of Bioenergy and Bioprocess Technology, Chinese Academy of Sciences, 189 Songling Road, Laoshan District, Qingdao, Shandong 266101, P. R. China.
[2] Laboratoire Catalyse & Spectrochimie, Normandie Univ, ENSICAEN, UNICAEN, CNRS, 6 Marechal Juin, 14050 Caen, France.

Keywords: hierarchical zeolite, in situ etching, mother liquor, metastability, MTO

Fabrication of hierarchical porosity in microporous zeolites is a key to overcome the inherent mass-transfer limitation and to improve the molecular accessibility to the active sites. The present study reports a facile and cost-effective etching strategy based on the crystal metastability to construct hierarchical SAPO-34 (**CHA**-type) zeolite. The hierarchical SAPO-34 with high crystallinity is obtained conveniently via an extended hydrothermal treatment without using any additional chemicals. The crystal etching is triggered by the metastability of SAPO-34 in the mother liquor. The hierarchical characteristics of etched SAPO-34 are found dependent on the crystallization-dissolution process controlled by the synthesis temperature and time. The products are systematically investigated by complementary characterization methods providing information on the textural properties and chemical environments of framework atoms. The resultant hierarchical zeolites exhibit improved diffusion and accessibility to the active sites in the micropores. Consequentially, the

hierarchical SAPO-34 zeolite shows remarkably enhanced catalytic performance in the methanol-to-olefin (MTO) reaction, compared with the microporous counterpart. The present approach to hierarchical zeolites could be extended to tailor the properties of other zeo-types.

1. Introduction

Zeolites are inorganic microporous crystalline materials widely applied in catalysis, adsorption, and separation processes.[1] The uniform channels or cavities of the molecular dimension offer confined space for the molecules reacting inside, thus endowing the zeolites' shape selectivity. The steric constraints of zeolite porosity can screen reactants and/or products that diffuse into or out of the zeolites by their molecular sizes.[2] This shape selectivity is a unique zeolite feature distinct from other heterogeneous catalysts and has been extensively applied in the petrochemical and fine-chemical catalytic processes. The well-defined pore structure of the zeolite, on the one hand, can afford high selectivity to the molecules with suitable molecular dimensions. However, on the other hand, the small pore size and long diffusion path length decrease the mass transport and cause severe coke deposition, resulting in low utilization efficiency and reduced catalytic performance of zeolites. Therefore, continuous efforts have been devoted to improving the diffusion in zeolites, besides maintaining their high selectivity and catalytic activity.[3] In the past decades, the fabrication of hierarchical zeolites with two or three levels of porosity integrating intrinsic micropores has been proven to be an effective strategy for overcoming the diffusion constraints.

Various approaches have been developed to prepare hierarchically porous zeolites, such as mesoporogen-directed method (hard- and soft-templating),[4] mesoporogen-free method (seed-assisting and kinetical regulation, etc.),[5] and post-treatment method (steam treatment, acid or alkali etching, fluoride etching, etc.).[6] Nevertheless, the use of expensive reagents, complicated procedures, and substantial mass loss for most synthetic approaches inhibit

potential commercial use. Specifically, the high cost, possible health, and environmental issues of organic mesoporogen may limit the industrial application of mesoporogen-directed method. The mesoporogen-free approach may lead to the low crystallinity and yield of hierarchical zeolites. Meanwhile, it would generate a substantial amount of defect sites that reduce their hydrothermal stability. Whereas the hierarchical zeolites prepared by post-treatment approaches generally suffer from severe damage of crystal and mass loss. Therefore, it remains an enormous challenge to develop facile, energy-efficient, and cost-effective synthetic strategies to construct hierarchical zeolites with abundant meso-/macropores, minimal mass loss, and high hydrothermal stability.

The zeolites are metastable materials, and the variation of any of the synthetic variables may lead to changing the chemical equilibrium and, thus to dissolution or phase transformation.[7] An already formed zeolite which is not in equilibrium with the mother liquor, is foredoomed to dissolution. Therefore, the metastability renders zeolites promising potential in pore architecture engineering, which was not used up to now.

Silicoaluminophosphate SAPO-34 with **CHA** topology,[8] has proven to be a highly efficient industrial catalyst for the production of ethylene and propylene by the methanol-to-olefin (MTO) reaction.[9] However, the intrinsic diffusion limitation of SAPO-34 restrains mass transport and cause severe coke deposition, thereby leading to rapid catalyst deactivation.[9b, 10] As mentioned, the generation of hierarchical architecture by post-synthetic etching is a simple, cost-effective and efficient strategy to improve mass-transfer in zeolites.[3b, 3c, 6a] However, it is challenging to tailor SAPO-34 zeolites using conventional acid/base leaching, mainly due to the less stable framework of SAPOs than that of the aluminosilicate zeolites. The difficulty comes from the framework alternation of aluminium and phosphorus, i.e., the preferential extraction of one of them leads to structural collapses. Therefore, it is indispensable to exploit an etching strategy that endows the indiscriminate

leaching, yet retains the framework structure and crystallinity of SAPO-34. Inspired by the metastability of zeolites,[11] when they are not in equilibrium with the mother liquor, we have developed a one-pot synthesis and etching approach. The generation of mesopores is achieved by a simple extension of the crystallization time over crystal growth reaction. Additionally, the hierarchical characteristics of mesoporous SAPO-34 zeolites can be modified by regulating the treatment temperature. The zeolite, in our case SAPO-34, starts to dissolve without destabilizing the framework and substantially varying the framework composition. Thus, the generation of a hierarchical material is controlled by the time and the temperature, and the zeolite remains in non-equilibrium with mother liquor.

Herein we report a straightforward, environmentally benign and economical *in situ* etching strategy to prepare hierarchical SAPO-34 zeolites with high crystallinity and limited mass loss. The synergy between crystallization and dissolution of SAPO-34 crystal in mother liquor for constructing hierarchical architecture is highlighted and discussed, according to the systematic characterization of textural properties and chemical compositions of SAPO-34 zeolites. The resultant hierarchical SAPO-34 zeolite shows remarkably enhanced catalytic performance with long catalytic lifetime and increased selectivity to ethylene and propylene in MTO reactions.

2. Results

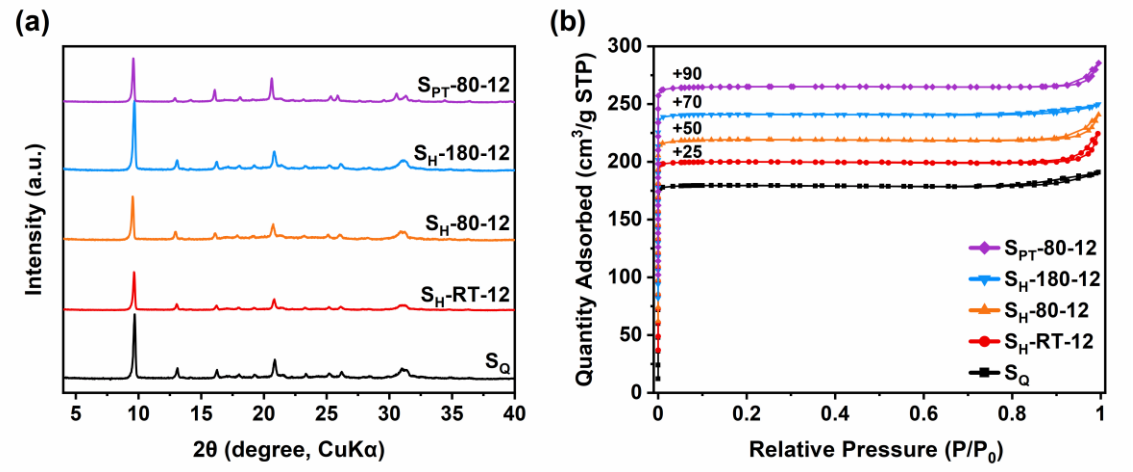

Figure 1. (a) Powder XRD patterns and (b) nitrogen adsorption-desorption isotherms of the as-synthesized SAPO-34 samples.

The XRD patterns of the as-prepared samples are displayed in **Figure 1**(a) and **Figure S1.** Notably, S_H-*x*-*y* samples were obtained by *in situ* etching with mother liquor. S_{PT}-80-12 was prepared by post-treatment with triethylamine (TEA) aqueous solution, and S_Q sample was obtained by quenching the autoclave immediately after synthesis. All samples exhibit the characteristic peaks of **CHA**-type structure. No additional peaks or obvious amorphous halos are observed from the XRD patterns, indicating that all samples are crystalline after quenching and subsequent etching in the mother liquor. The peaks intensity of S_H-RT-12, is lower than S_Q sample, revealing a partial dissolution of crystals remaining in the mother liquor at room temperature (RT) for 12 h, which is an expected consequence of the SAPO-34 metastability. The crystallinity of S_H-80-12 and S_H-180-12 samples is higher than S_H-RT-12 (**Table 1** and **Table S1**, in the Supporting Information), which points out that upon hydrothermal treatment a new equilibrium in the system leading to a secondary growth of crystal was reached. The crystallinity of material treated at 180 °C (S_H-180-12) is even higher than the reference S_Q sample. This result shows that the equilibrium growth of SAPO-34 is temperature-dependent. Thus, the crystals obtained at a particular temperature could undergo dissolution (S_H-80-12) or secondary growth (S_H-180-12) as a function of temperature. The mass analysis of treated samples supported the above conclusion. The mass of S_H-RT-12 is 79% of the S_Q reference (Table 1), revealing a certain level of dissolution. The material subjected to hydrothermal treatment at 80 °C (S_H-80-12) showed a mass gain (92 wt.%) with respect to S_H-RT-12. A similar result was obtained at 180 °C as the mass of the sample (S_H-180-12) was even higher than the reference S_Q (112 wt.%), as shown in Table 1 and Table S1. Therefore, the analysis of the mass of treated samples corroborates the XRD study (Table 1).

N_2 adsorption-desorption analysis was performed to study the porous and textural properties of the SAPO-34 samples. As shown in Figure 1(b), all samples exhibit the type I

isotherm characteristic of microporous materials. A second uptake near saturation pressure ($P/P_0 > 0.8$) indicative of the presence of mesopores was observed for S_H-RT-12 and S_H-80-12 samples (Figure 1b).[12] The surface and porous characteristics of all SAPO-34 samples are summarized in Table 1 and **Table S2**. The hierarchical SAPO-34 samples (S_H-RT-12 and S_H-80-12) show decreased micropore volumes (0.26 $cm^3\ g^{-1}$, 0.26 $cm^3\ g^{-1}$) in comparison with the S_Q and S_H-180-12 materials (0.27 $cm^3\ g^{-1}$, 0.27 $cm^3\ g^{-1}$). The decrease in micropore volumes is in line with the decreased crystallinity measured by XRD. Meanwhile, an increase in the external surface area (S_{ext}) and mesopore volume (V_{meso}) of samples S_H-RT-12, S_H-80-12, and S_{PT}-80-12 is observed, which results from the introduced secondary porosity. The pore size distributions, as shown in **Figure S2**, prove the obvious presence of mesopores (ca. 20 nm).

Table 1. Framework composition, sample mass, X-ray crystallinity, and textural properties of the hierarchical SAPO-34 samples compared with the reference sample.

Sample	Molar compositions [a]	Mass [b] (%)	Relative crystallinity [c] (%)	S_{BET} [d] ($m^2\ g^{-1}$)	S_{ext} [e] ($m^2\ g^{-1}$)	V_{micro} [e] ($cm^3\ g^{-1}$)	V_{meso} [f] ($cm^3\ g^{-1}$)
S_Q	$Si_{0.08}Al_{0.49}P_{0.43}O_2$	100	100.0	534	9	0.27	0.02
S_H-RT-12	$Si_{0.09}Al_{0.48}P_{0.43}O_2$	79	58.7	558	15	0.26	0.04
S_H-80-12	$Si_{0.08}Al_{0.50}P_{0.42}O_2$	92	70.0	583	32	0.26	0.04
S_H-180-12	$Si_{0.07}Al_{0.48}P_{0.45}O_2$	112	102.4	524	5	0.27	0.01
S_{PT}-80-12	$Si_{0.09}Al_{0.48}P_{0.43}O_2$	57	45.0	574	58	0.24	0.03

[a] Measured by an inductively coupled plasma (ICP) spectrometer. [b] Mass = M2/M1, wherein M1 is the mass of the zeolite product without treatment (S_Q), M2 is the mass of the sample after etching. [c] Relative crystallinity was calculated by relative peak (2θ = 9.3–9.4, 15.8, and 20.4 °) intensity in the XRD pattern. [d] S_{BET} (total surface area) was calculated by applying the BET equation using the linear part ($0.05 < P/P_0 < 0.30$) of the adsorption isotherm. [e] S_{ext} (external surface area) and V_{micro} (micropore volume) were calculated using the *t*-plot method. [f] V_{meso} (mesopore volume) calculated using the BJH method (from desorption).

The morphology of the treated SAPO-34 samples is studied by combining scanning (SEM) and transmission electron microscopy (TEM). The SEM images of the as-synthesized SAPO-34 sample is shown in **Figure S3**. SAPO-34 crystals exhibit the typical for this material pseudo cubic morphology with an average particle size of about 2 μm. Compared

with S_Q sample, the S_H-RT-12 samples show a rough surface with many holes, which results from the *in situ* mother liquor dissolution, as evidenced by the analysis of textural properties. Notably, the etching temperature increase to 80 °C (S_H-80-12) results in a symmetric cross-shaped dissolution profile. Furthermore, larger and deeper pores are observed in the SAPO-34 crystals upon prolonged (S_H-80-24) treatment at 80 °C (Figure S3(f) in the Supporting Information). On the other side, we found out that the sample gained in mass upon treatment at 80 °C (Table 1). Therefore, the phenomena of both dissolution and growth take place at this temperature. Based on the mass gain, we conclude that the dominant process is secondary growth. This phenomenon is more pronounced at higher treatment temperatures. Upon treatment at temperatures higher than 100 °C, the etched regions gradually diminish and eventually disappear upon treatment at 180 °C (Figure S3(i) in the Supporting Information), signifying that the crystallization outperforms the dissolution in this temperature range.

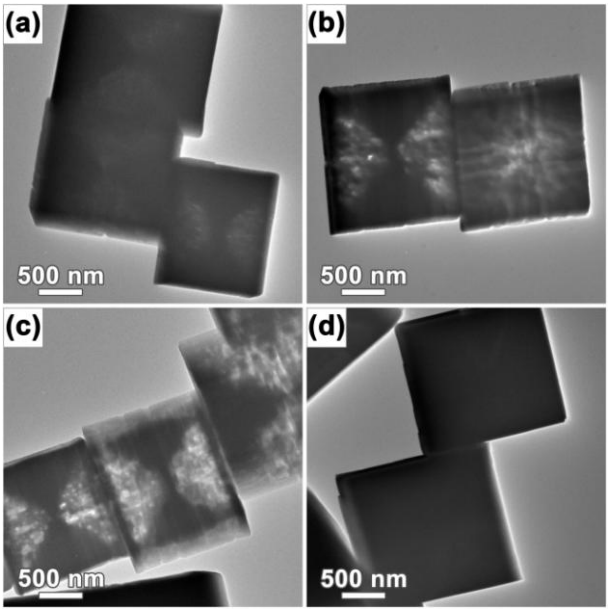

Figure 2. TEM images of as-synthesized SAPO-34 samples (a) SQ, (b) S_H-RT-12, (c) S_H-80-12, (d) S_H-180-12.

TEM provides further insights into the structure and morphology of the series of SAPO-34 samples (**Figure 2** and **Figure S4** in the Supporting Information). The light and shade contrast symmetric cross-shaped structures of etched SAPO-34 samples reveal zones with

different density in the materials. As shown in Figure 2(a), the S_Q sample exhibits the symmetric cross-shaped structures with low dark-to-light contrast. This result shows that the synthesis time was too long, and the crystals were already in non-equilibrium conditions. This process was accentuated after cooling down and keeping the crystals at RT for 12 h (Figure 2b). Four of the crystal faces are preferentially dissolved, which generates a structure resembling a "sand-watch". The exact phenomenon staying behind the dissolution profile is not known. However, our previous studies revealed that the defect zones in zeolite control to a great extent, the dissolution process.[13] In accordance with the N_2 adsorption-desorption analysis, the secondary larger pores observed by TEM and SEM correspond to the extra mesopores (ca. 20 nm) and macropores (ca. 60 nm) in S_H-RT-12 and S_H-80-12 crystals. It is worth noting that, when the *in situ* etching temperature is higher to 80 °C, the symmetric cross-shaped structure gradually diminishing and disappears after treatment at 180 °C (Figure S4 in the Supporting Information). No large secondary pores are observed on the S_H-180-12 sample. This is in line with the results of XRD patterns and SEM images, which further confirms the recrystallisation of SAPO-34.

The compositions of resulting SAPO-34 samples determined by ICP-OES are given in Table 1 and Table S1. The etched samples (S_H-RT-12, S_H-80-12, and S_H-180-12) show the comparable framework compositions with S_Q. The results demonstrate that the mother liquor etching is non-selective towards a particular framework cation. Thus, the unbiased chemical dissolution generates a hierarchical material with a composition similar to the parent.

Table 2. Textural properties of the recrystallized and post-treated SAPO-34 catalysts.

Sample	S_{BET} ($m^2\ g^{-1}$)	S_{ext} ($m^2\ g^{-1}$)	V_{micro} ($cm^3\ g^{-1}$)	V_{meso} ($cm^3\ g^{-1}$)
S_R-60-24	625	36	0.24	0.03
S_R-80-24	633	71	0.25	0.07
S_R-120-24	547	19	0.25	0.03
S_R-180-24	527	7	0.26	0.01

The above analyses manifest that the mother liquor etching can effectively tailor a hierarchical architecture. The hierarchical characteristics correlate with the dissolution and secondary growth processes in the mother liquor, which is dependent on the etching temperature and time.

Mother liquor etching was compared with a conventional post-synthesis etching of SAPO-34 using aqueous triethylamine (TEA) solution as an etching agent. SAPO-34 was subjected to etching in aqueous TEA solution at 80 °C for 12 h (S_{PT}-80-12). As can be seen in Table 1, both the yield and crystallinity of S_{PT}-80-12 are lower than that of S_H-80-12 sample etched in the mother liquor under similar temperature-time conditions. The V_{micro} of TEA post-treated S_{PT}-80-12 (0.24 cm^3 g^{-1}) is lower than that of S_H-80-12 (0.26 cm^3 g^{-1}) (**Table 2**). The crystallinity of S_{PT}-80-12 is also lower than S_H-80-12 (Figure 1a). The TEM image of S_{PT}-80-12 in Figure 4(d) shows that the crystals are deeply etched and even fragmented to small pieces. Briefly, the aqueous TEA aqueous solution etching is much more aggressive than mother liquor's one, leading to substantial crystallinity and mass losses. Thus, TEA which is a structure-directing agent for SAPO-34 acts as an etching agent when the crystals are not in equilibrium with mother liquor.[14] The dissolution and growth behavior of SAPO-34 in the mother liquor is investigated by subjecting the RT etched sample (S_H-RT-12) to treatment at different temperatures for 24 h. The XRD patterns of the as-synthesized samples (S_R-60-24, S_R-80-24, S_R-120-24 and S_R-180-24) are given in **Figure 3**(a). Compared with S_H-RT-12, the samples S_R-60-24 and S_R-80-24

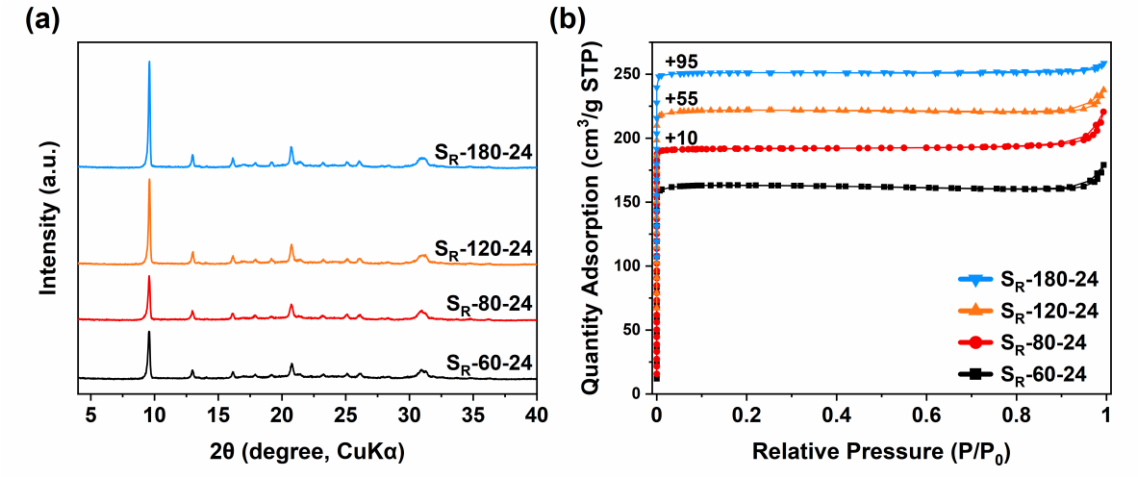

Figure 3. (a) Powder XRD patterns and (b) Nitrogen adsorption-desorption isotherms of the recrystallized SAPO-34 samples.

are etched more deeply. Larger pores penetrate into the crystal core, as some sections of the crystals are segmented (**Figure 4**(a), Figure S4(f), and **Figure S5**(a)-(b) in the Supporting Information). However, as shown in Figure 4(b)-(c) and Figure S5(c)-(d), the crystals are recovered with freshly grown layer when the hydrothermal treatment temperature is raised to 120 °C and 180 °C. The reduction of the extra larger pores is in line with the decrease in the external surface area (S_{ext}) (Figure 3b and Table 2). Notably, the mass gain and relative crystallinity of the samples (S_R-60-24, S_R-80-24, S_R-120-24, and S_R-180-24) increase with the

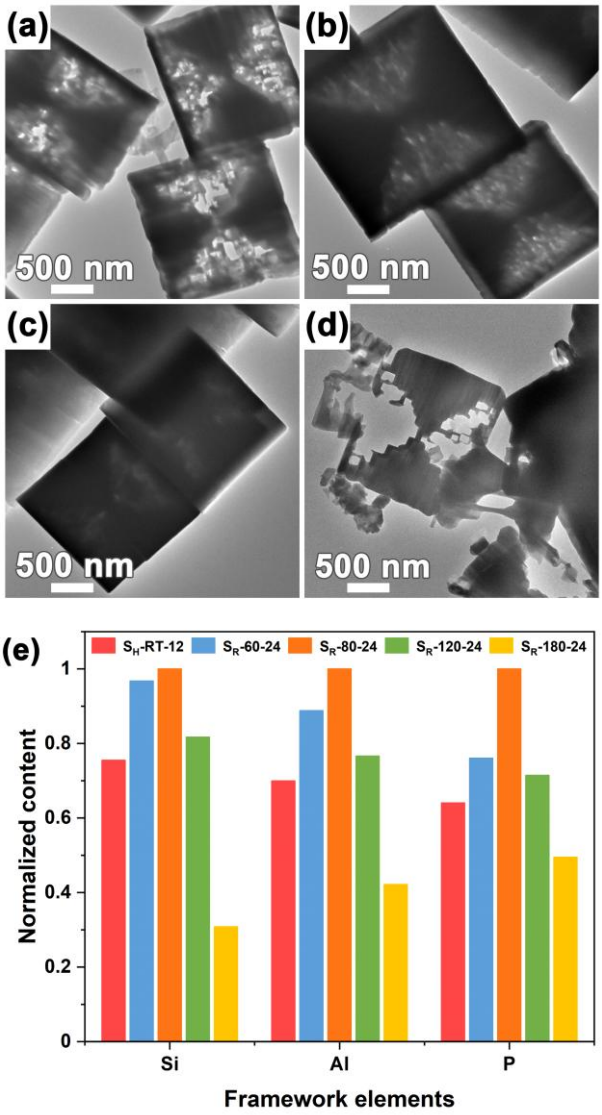

Figure 4. (a)-(d) TEM images of SAPO-34 samples S_R-60-24, S_R-120-24, S_R-180-24 and S_{PT}-80-12, and (e) Normalized Si, Al and P contents in the mother liquor of S_R samples.

rise of the temperature (**Table S3**, in the Supporting Information). We further investigated the evolution of crystals at 180 °C for different treatment periods. As shown in Figure S5(e)-(g), the secondary pores on samples S_R-180-3, S_R-180-6, and S_R-180-12 gradually diminish with the increase of treatment time.

The liquid compositions of the mother liquors were analyzed by the ICP-OES to elucidate the dissolution and etching processes of SAPO-34. The high content of framework elements in the liquid phase implies that the crystal has been dissolved by the mother liquor, while the low content indicates the consumption of the framework ingredients by crystal

growth. As can be seen, the framework ingredients in the mother liquor are consumed at a temperature higher than 80 °C, indicating that a recrystallisation process takes place in the system (Figure 4e). These results demonstrate the dynamic equilibrium in the system that can switch the process from growth to dissolution and *vice versa*.

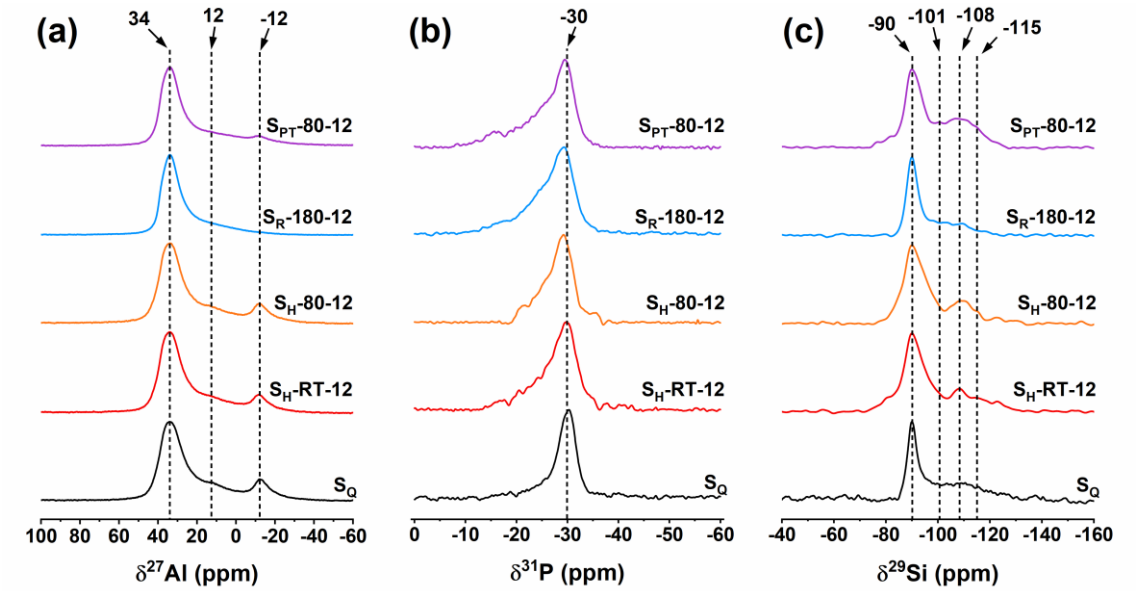

Figure 5. (a) ^{27}Al, (b) ^{31}P and (c) ^{29}Si solid-state MAS NMR spectra of as-prepared SAPO-34 samples.

Solid-state ^{27}Al, ^{29}Si and ^{31}P MAS NMR spectroscopy were employed to probe the chemical environments of framework atoms in the hierarchical SAPO-34 samples. In **Figure 5**(a), the ^{27}Al MAS NMR signals at 34 ppm are attributed to tetrahedrally coordinated framework aluminium atoms.[15] The weak signals at 12 ppm attribute to penta-coordinated aluminium atoms, while the weak peak at ca. -12 ppm is assigned to the octahedral extra-framework aluminium atoms.[15a, 16] The ^{27}Al MAS NMR spectra of S_Q, S_H-RT-12, and S_H-80-12 samples are comparable. While S_R-180-12 sample shows different ^{27}Al MAS NMR spectrum, in which the signals at about 12 ppm and -12 ppm are almost invisible. In combination with TEM and textural analysis, the ^{27}Al MAS NMR analysis of S_R-180-12 manifests that the recrystallisation may lead to the transformation of penta- and hexa-coordinated aluminium species into the framework. Compared with S_Q, the post-treated

sample S_{PT}-80-12 exhibit weaker peaks at about 12 ppm and -12 ppm, suggesting that post-etching results in the partial removal of penta-coordinated aluminium atoms and octahedral aluminium atoms. ^{31}P MAS NMR spectra are shown in Figure 5(b), indicating that tetrahedrally coordinated phosphorus is present in the SAPO-34 samples based on the signal at about -30 ppm.[15a, 17]

In the ^{29}Si MAS NMR spectra (Figure 5c), the signals at about -90 ppm originating from the coordination state of Si(0Si4Al) show high intensity in all measured SAPO-34 samples.[18] The signals at around -101 ppm are ascribed to the coordination state of Si(2Si2Al).[17, 19] It is worth noting that the sample S_R-180-12 exhibits the weaker peaks at -108 and -115 ppm than that of the other samples, suggesting that less Si(3Si1Al) and Si(4Si0Al) species exist in the S_R-180-12 sample due to the further regrowth process. The analysis of ^{29}Si MAS NMR on S_R-180-12 is in accord with the result of ^{27}Al MAS NMR. Moreover, it can be seen that the Si(4Si0Al) species in the resulting hierarchically SAPO-34 (S_H-RT-12, S_H-80-12 and S_{PT}-80-12) apparently decrease compared with the sample S_Q, implying that both the *in situ* etching in the mother liquor and post-treatment in TEA aqueous solution could lead to a decrease of Si-island species.

Summarizing these results, one can state that the dissolution-regrowth of SAPO-34 in the mother liquor provides a unique opportunity to tune the hierarchical characteristics of the material. The major stages of the process are summarized in Scheme 1. As shown, the mother liquor contains TEA, silicon, phosphorus, and aluminium species, which originate from the unreacted raw material or are extracted from the crystals during the etching process. These components play the role of ingredients in the growth process; meanwhile, after passing the equilibrium threshold TEA act as an etching agent. At low temperature (RT), the etching process overwhelms the crystallization, generating large secondary pores in crystals. Placing the system at a temperature higher than 80 °C switches the equilibrium from dissolution to

growth. Thus the etched crystal starts to grow and the generated mesopores start to close. Consequentially, the hierarchical pores in the etched samples disappeared upon high-temperature hydrothermal treatment. At 180 °C, the regrowth generates a SAPO-34 with crystallinity higher than the parent synthesized at 200 °C. This result shows that 180 °C is a temperature more appropriate for the synthesis of SAPO-34.

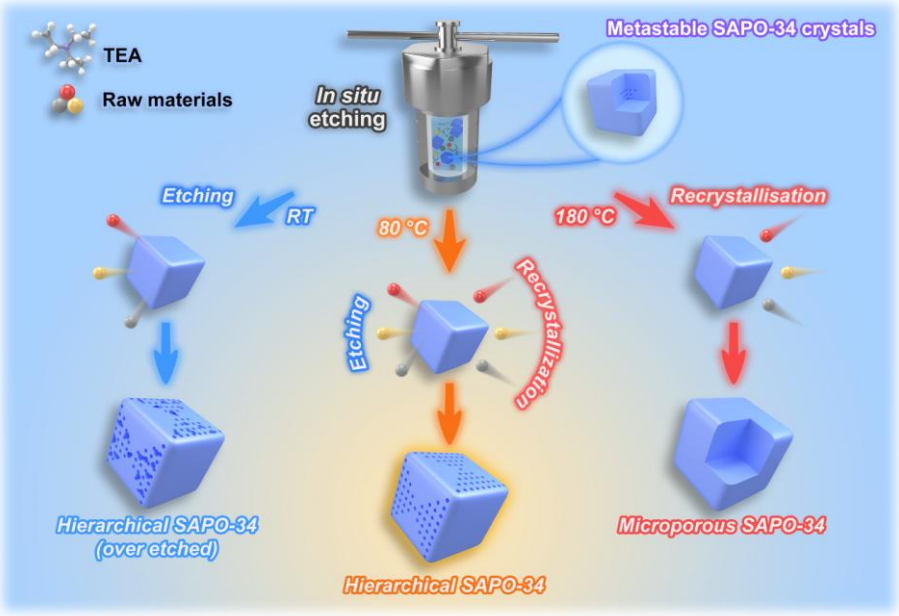

Scheme 1. Metastable behavior of SAPO-34 in the mother liquor as a function of the temperature.

The NH_3-TPD profiles of the prepared SAPO-34 samples are presented in **Figure 6**(a). Two ammonium desorption peaks centered at about 182 °C and 422 °C represent the weak and strong acid sites in the SAPO-34 zeolites.[20] The desorption peaks corresponding to weak acid sites are comparable for all the measured samples. While the post-treated sample by aqueous TEA solution (S_{PT}-80-12) shows a peak ascribing to strong acid sites at around 390 °C, which is lower than that at around 422 °C for other SAPO-34 samples. The desorption peak at lower temperature indicates relatively weaker acidity. The ammonium desorption profiles manifest that the acidity of S_{PT}-80-12 sample is weaker after aqueous TEA solution etching. It signifies that the later treatment damages the framework, thus leading to a decrease of acidity. It is noteworthy that the ammonia desorption profiles of S_H-80-12 are

similar to that of S_Q, implying that the acidity of hierarchical S_H-80-12 samples hardly changed after *in situ* etching at 80 °C. The fact that S_H-80-12 retaining the acidic properties is attributed to the indiscriminate extraction of framework atoms and largely preserved crystallinity under mother liquor etching.

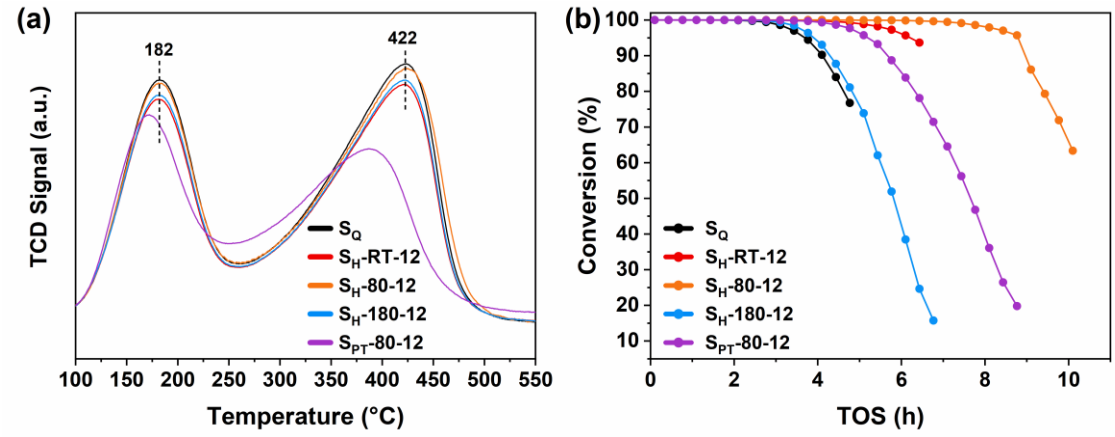

Figure 6. (a) NH_3-TPD profiles of the counterpart and hierarchical SAPO-34 samples. (b) Methanol conversion variation with time-on-stream over the SAPO-34 catalysts with different etching conditions. Experimental conditions: WHSV = 2 h^{-1}, T = 400 °C, catalyst weight = 100 mg.

The MTO reaction was applied to evaluate the catalytic performance of the prepared SAPO-34 catalysts at 400 °C with WHSV of 2.0 h^{-1}. The conversion of methanol with the time on stream is given in Figure 6(b) and **Figure S6**. As shown, the methanol conversion reaches 100% at the beginning of the reaction. The catalytic lifetime, with 100% conversion of methanol, of the hierarchical sample S_H-80-12, has been hugely prolonged and reached up to 5.8 h, which is nearly 3-folds of that over S_Q (2.1 h) and 3-folds of that over the bulky crystal S_{SEED} (1.8 h). The superior catalytic performance of S_H-80-12 sample is ascribed to the introduction of secondary pores, which largely enhance the transport efficiency. The hierarchical pore structures in the SAPO-34 catalysts can effectively circumvent the diffusion limitation and retard coking, thereby leading to a prolonged lifetime. Noticeably, the lifetime of sample S_H-180-12 (2.4 h) is comparable with the parent sample (S_Q). It is attributed to the absence of secondary pores in S_H-180-12 due to the dominant recrystallisation process at

180 °C. As exhibited in **Table S4** and **Figure S7**, the selectivity of ethylene and propylene of sample S_H-80-12 (83.81%) is 11.1% higher than the S_{SEED} sample (72.74%).

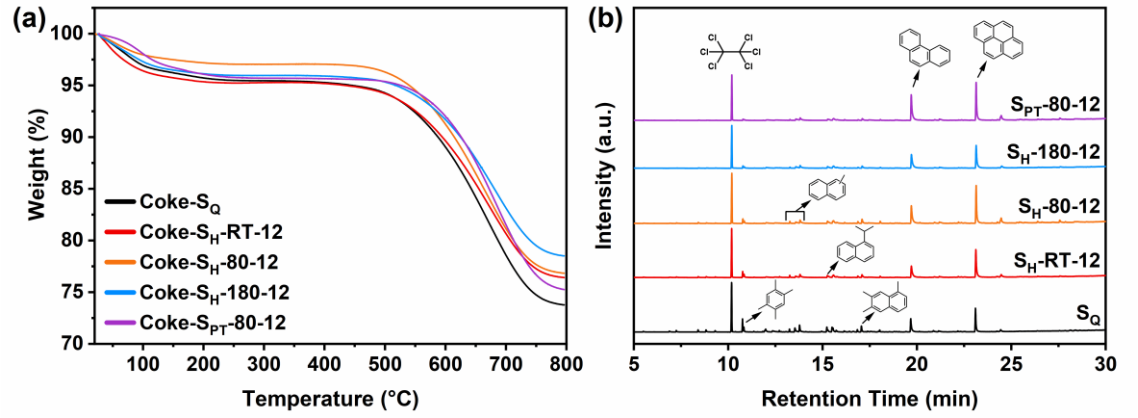

Figure 7. (a) TG curves of the SAPO-34 catalysts. (b) GC-MS chromatograms of organic coke species in the catalysts after methanol conversion at 400 °C. The structures annotated onto the chromatograms are peak identifications in comparison with the mass spectra to those in the NIST database, and hexachloroethane (C_2Cl_6) was the internal standard.

After the reaction, the used SAPO-34 samples were analyzed by TG to evaluate the coke content (**Figure 7**a and **Table S5**). The coke species were identified by GC-MS and shown in Figure 7(b). As shown in Table S5, the rate of coke deposition of sample S_H-80-12 is only 0.06 mg min^{-1}, which is much lower than that of the other samples. The abundant meso- and macropores in the catalyst enhance the diffusion and retard coke deposition. Moreover, compared with the hierarchical samples, there is more coke deposited on the sample S_Q. As is illustrated in Figure 7(b), the amount of bulky polycyclic aromatics, such as phenanthrene, pyrene, and their derivatives in the sample S_H-80-12 are obviously larger than that of the sample S_Q. It indicates that the meso- and macropores in hierarchical SAPO-34 catalysts are of great importance in accommodating bulky coke species. Due to hierarchical structures constructed by *in situ* etching in the SAPO-34 zeolites, the active sites in the microporous space are more accessible and mass transfer is improved, thereby restraining the rapid coke deposition during methanol conversion. Consequently, the hierarchical SAPO-34 sample shows a largely extended lifetime and boosted selectivity to C_2H_4 and C_3H_6 in MTO reactions.

3. Conclusion

In summary, a simple, environmentally benign and economical etching approach to generate hierarchical zeolites was reported. The approach, exemplified by the preparation of hierarchical SAPO-34, is based on the zeolite metastability. After the completion of zeolite crystallization, the extension of treatment time or shifting the system to a lower temperature places the zeolite in a non-equilibrium state, and thereby a partial dissolution process starts. This way, based on metastability, which is a fundamental zeolite characteristic, a hierarchical pore structure can be obtained. It was found that the metastability is temperature dependent reaction, as the SAPO-34 crystal dissolution takes place at low temperature (RT to 80 °C). In comparison, at high temperature (100 to 180 °C) the etched crystals regrow. Therefore, selecting a specific crystallization temperature, then cooling down to RT and heating up again, allows engineering the zeolite hierarchical pore architecture. This is achieved without using additional chemicals or treatment steps. The present study provides a simple, straightforward, and environmentally method for preparing hierarchic porous structures, which can be applied to different zeo-types.

4. Experimental Section

4.1. Reagents

The following reagents were employed: phosphoric acid (H_3PO_4, 85 wt.%, Beijing Chemical Reagent Company), pseudo-boehmite (Al_2O_3, 62.5 wt.%, Vista Company), triethylamine (TEA, 99 wt.%, Fuyu Company), colloidal silica (SiO_2, 40 wt.%, Sigma-Aldrich Company). Ultrapure water was obtained with the Merck Milli-Q Ultra-Pure Water System.

4.2. Synthesis

Synthesis of SAPO-34 zeolite seeds: The molar composition of the reaction mixture was set to $0.3SiO_2$: $1.0Al_2O_3$: $1.1P_2O_5$: 4.5TEA: $70H_2O$. Specifically, H_3PO_4 and ultrapure water were

mixed, then pseudo-boehmite was added to the above mixture. After stirring for 1 h at room temperature, TEA was added dropwise into the mixture, followed by continuous stirring for another 1 h. Finally, colloidal silica was added dropwise into the synthesis gel. The reaction mixture was further stirred for 3 h and then was transferred into a 100 mL Teflon-lined stainless-steel autoclave. The crystallization proceeded in a conventional oven at 200 °C for 24 h. The as-synthesized solid product was centrifuged, washed with water, and then dried at 90 °C in an oven overnight, followed by calcination at 600 °C for 8 h and was denoted as S_{SEED}.

Preparation of quenched SAPO-34 zeolite: The molar composition of the reaction mixture was set to $0.3SiO_2$: $1.0Al_2O_3$: $1.1P_2O_5$: 4.5TEA: $70H_2O$: 8.0 wt.% seed. The synthesis procedure was similar to that for S_{SEED}, except an additional introduction of 8.0 wt.% S_{SEED} into the synthesis mixture. Seeds were employed to obtain smaller crystals. The synthetic gel was then transferred into 20 mL Teflon-lined stainless-steel autoclaves with static crystallization at 200 °C for 24 h. Afterwards, the reaction system was quenched immediately. And the solid product was centrifuged, washed, and calcined. The resulting product denoted as S_Q was used as a reference sample.

Synthesis of hierarchical SAPO-34 zeolites by in situ etching in mother-liquor: The series of S_H samples were prepared by transferring quenched autoclaves of S_Q to the ovens at different temperatures. Specifically, after obtaining the quenched autoclaves contained S_Q sample, the quenched autoclaves were transferred to the ovens at temperatures from room temperature to 180 °C for 3–24 hours. After that, the as-synthesized solid products were centrifuged and washed with water, then dried at 90 °C overnight, followed by calcination at 600 °C for 8 h. The prepared samples were denoted as S_H-*x*-*y*, in which symbol *x* refers to the *in situ* etching temperature and *y* represents the treatment time in hours, respectively.

Preparation of hierarchical SAPO-34 zeolite by post-treatment in TEA aqueous solution: For comparison, the conventional post-treatment approach was used to prepare hierarchical SAPO-34 sample. The parent sample used for TEA post-etching was obtained following the protocol of synthesis of the above sample $S_{Q,}$ but without calcination. Specifically, 1.4 g of the parent sample was added into the TEA aqueous solution, which contains 2.68 g of TEA and 8.08 g of ultrapure water. The mixture was transferred into 20 mL Teflon-lined stainless-steel autoclave and maintained at 80 °C for 12 h. The solid product, denoted S_{PT}-80-12, was centrifuged, washed, dried, and calcined.

Preparation of recrystallized SAPO-34 zeolites by further in situ etching S_H-RT-12: The series of S_R samples were prepared for the investigation of recrystallisation process in the mother liquor. Specifically, the *in situ* etching procedure was similar to that of series of S_H samples, except that the parent sample is not S_Q but S_H-RT-12. After quenching and keeping at RT for 12 h (S_H-RT-12), the obtained autoclaves were subsequently put back into the oven at 60 °C, 80 °C, 120 °C, and 180 °C for another 24 hours. The prepared solid was sequentially centrifuged, washed, dried at 90 °C overnight, and calcined at 600 °C for 8 h. The obtained samples were donated as S_R-*a*-*b*, in which R refers to the recrystallized samples, and symbol *a* and *b* represent for the temperature and duration of recrystallisation, respectively.

4.3. Characterization

The phase analysis and crystallinity of SAPO-34 samples were studied by powder X-ray diffraction operated on a Rigaku DMax-2550 diffractometer with Cu Kα radiation (λ = 1.5418 Å). The crystal morphology and size were studied with field emission scanning electron microscopy (SEM) and transmission electron microscopy (TEM), operating on the JSM-7800F, JSM-7610F, and Tecnai F20 electron microscopy, respectively. The compositions of samples were analyzed with inductively coupled plasma-optical emission spectrometry (ICP-OES), carried out on a PerkinElmer Optima 3300 DV ICP instrument. Nitrogen adsorption-

desorption measurements were carried out on the Micromeritics 2020 analyzer at 77.35 K after the samples were degassed at 350 °C under vacuum for 10 h. The acidic properties of samples were tested by temperature-programmed desorption of ammonia (NH_3-TPD) on a Micromeritics AutoChem II 2920 automated chemisorption analysis unit with a thermal conductivity detector (TCD) under helium flow. ^{29}Si MAS NMR, ^{27}Al MAS NMR, and ^{31}P MAS NMR experiments were performed on a Bruker Avance III/WB-400 spectrometer using a 4-mm MAS probe at a spinning rate of 12 kHz, corresponding to a frequency of 79.50 MHz.

4.4. Catalytic Test and Carbon Deposition Analysis

The MTO reaction was carried out in a quartz tubular fixed-bed steel reactor with a length of 30 cm and an inner diameter of 6 mm under atmospheric pressure. 0.1 g (40–60 mesh) catalyst of calcined SAPO-34 sample was packed in the center of quartz wools. The sample was pre-treated in N_2 flow of 30 mL min^{-1} at 500 °C for 1 h, and then the temperature of the reactor was adjusted to 400 °C. The reactant methanol was fed by a carrier gas (N_2, 10 mL min^{-1}) through a saturator containing methanol at 40 °C, which gave the estimated weight hourly space velocity (WHSV) of 2.0 h^{-1}. The reaction products were analyzed by an on-line gas chromatograph (Agilent GC 7890N) equipped with flame ionization detector (FID) and Plot-Q capillary column (Agilent J & WGC Columns, HP-PLOT/Q19091P-Q04, 30 m × 320 μm × 20 μm). The conversion and selectivity were calculated on CH_2 basis.

The amount of generated coke in SAPO-34 catalysts after the MTO reactions was determined by thermal analysis (TG) on a TGA Q500 at a heating rate of 10 °C min^{-1} from room temperature to 800 °C under airflow. To analyze the coke species, the exhausted SAPO-34 catalysts were etched in a HF solution for 24 h and then extracted by dichloromethane (CH_2Cl_2). Subsequently, the obtained solutions with the hexachloroethane (C_2Cl_6) as an internal standard were analyzed by a gas chromatograph equipped with a mass sensitive

detector (GC-MS). (Thermo Fisher Trace ISQ, equipped with TG-5MS column, 60 m × 320 μm × 25 μm).

Supporting Information

Supporting Information is available from the Wiley Online Library or from the author.

Acknowledgements

J. Han and G. Yang contributed equally to this work. This work is supported by the National Natural Science Foundation of China (Grant 21971082 and 22001090), and the Jilin Province Science and Technology Development Plan (Grant 20190201229JC and 20200201096JC). This work acknowledges the 111 Project (B17020). X.C. and V.V. acknowledge the collaboration in the framework of joint Sino-French international laboratory "Zeolites".

Received: ((will be filled in by the editorial staff))
Revised: ((will be filled in by the editorial staff))
Published online: ((will be filled in by the editorial staff))

References

[1] a) J. Li, A. Corma, J. Yu, *Chem. Soc. Rev.* **2015**, *44*, 7112; b) Y. Li, L. Li, J. Yu, *Chem* **2017**, *3*, 928; c) E. M. Gallego, M. T. Portilla, C. Paris, A. Leon-Escamilla, M. Boronat, M. Moliner, A. Corma, *Science* **2017**, *355*, 1051; d) T. De Baerdemaeker, D. De Vos, *Nat. Chem.* **2013**, *5*, 89.

[2] J. Kärger, R. Valiullin, *Chem. Soc. Rev.* **2013**, *42*, 4172.

[3] a) R. Bai, Y. Song, Y. Li, J. Yu, *Trends Chem.* **2019**, *1*, 601; b) G. Yang, J. Han, Y. Huang, X. Chen, V. Valtchev, *Chin. J. Chem. Eng.* **2020**, *28*, 2022; c) G. Yang, J. Han, Y. Liu, Z. Qiu, X. Chen, *Chin. J. Chem. Eng.* **2020**, *28*, 2227.

[4] a) Q. Sun, N. Wang, D. Xi, M. Yang, J. Yu, *Chem. Commun.* **2014**, *50*, 6502; b) C. J. H. Jacobsen, C. Madsen, J. Houzvicka, I. Schmidt, A. Carlsson, *J. Am. Chem. Soc.* **2000**, *122*, 7116; c) W. Fan, M. A. Snyder, S. Kumar, P.-S. Lee, W. C. Yoo, A. V. McCormick,

R. Lee Penn, A. Stein, M. Tsapatsis, *Nat. Mater.* **2008**, *7*, 984; d) M. Choi, H. S. Cho, R. Srivastava, C. Venkatesan, D.-H. Choi, R. Ryoo, *Nat. Mater.* **2006**, *5*, 718; e) R. Bai, Y. Song, R. Bai, J. Yu, *Adv. Mater. Interfaces* **2020**, https://doi.org/10.1002/admi.202001095, 2001095.

[5] a) Q. Zhang, A. Mayoral, O. Terasaki, Q. Zhang, B. Ma, C. Zhao, G. Yang, J. Yu, *J. Am. Chem. Soc.* **2019**, *141*, 3772; b) K. Ding, A. Corma, J. A. Maciá-Agulló, J. G. Hu, S. Krämer, P. C. Stair, G. D. Stucky, *J. Am. Chem. Soc.* **2015**, *137*, 11238; c) G. Yang, J. Han, Z. Qiu, X. Chen, Z. Feng, J. Yu, *Inorg. Chem. Front.* **2020**, *7*, 1975; d) Q. Sun, N. Wang, R. Bai, X. Chen, J. Yu, *J. Mater. Chem. A* **2016**, *4*, 14978.

[6] a) G. Yang, Z. Qiu, J. Han, X. Chen, J. Yu, *Mater. Chem. Front.* **2020**, *4*, 2982; b) X. Chen, A. Vicente, Z. Qin, V. Ruaux, J.-P. Gilson, V. Valtchev, *Chem. Commun.* **2016**, *52*, 3512; c) S. Du, X. Chen, Q. Sun, N. Wang, M. J. Jia, V. Valtchev, J. Yu, *Chem. Commun.* **2016**, *52*, 3580; d) V. Valtchev, S. Mintova, *MRS Bull.* **2016**, *41*, 689; e) Z. Qin, L. Hafiz, Y. Shen, S. Daele, P. Boullay, V. Ruaux, S. Mintova, J.-P. Gilson, V. Valtchev, *J. Mater. Chem. A* **2020**, *8*, 3621; f) V. Babić, L. Tang, Z. Qin, L. Hafiz, J.-P. Gilson, V. Valtchev, *Adv. Mater. Interfaces* **2020**, https://doi.org/10.1002/admi.202000348, 2000348.

[7] a) L. Jin, S. M. Auerbach, P. A. Monson, *J. Phys. Chem. C* **2010**, *114*, 14393; b) A. Erdem, *J. Catal.* **1979**, *60*, 241; c) F. Di Renzo, A. Albizane, M.-A. Nicolle, F. Fajula, F. Figueras, T. Des Courieres, in *Studies in Surface Science and Catalysis*, Vol. 65 (Eds: G. Öhlmann, H. Pfeifer, R. Fricke), Elsevier, 1991, 603.

[8] C. Baerlocher, L. McCusker, http://www.iza-online.org/, accessed: September 2020

[9] a) P. Tian, Y. Wei, M. Ye, Z. Liu, *ACS Catal.* **2015**, *5*, 1922; b) M. Yang, D. Fan, Y. Wei, P. Tian, Z. Liu, *Adv. Mater.* **2019**, *31*, 1902181; c) B. Yu, C. Lou, W. Zhang, S. Xu, J. Han, Z. Yu, Y. Wei, Z. Liu, *Chem. Res. Chin. Univ.* **2020**, https://doi.org/10.1007/s40242-020-0216-x.

[10] Q. Sun, Z. Xie, J. Yu, *Natl. Sci. Rev.* **2017**, *5*, 542.

[11] R. M. Barrer, *Zeolites and Clay Minerals as Sorbents and Molecular Sieves*, Academic Press, 1978.

[12] Z. Qin, L. Pinard, M. A. Benghalem, T. J. Daou, G. Melinte, O. Ersen, S. Asahina, J.-P. Gilson, V. Valtchev, *Chem. Mater.* **2019**, *31*, 4639.

[13] a) Z. Qin, L. Lakiss, J. P. Gilson, K. Thomas, J. M. Goupil, C. Fernandez, V. Valtchev, *Chem. Mater.* **2013**, *25*, 2759; b) Z. Qin, G. Melinte, J.-P. Gilson, M. Jaber, K. Bozhilov, P. Boullay, S. Mintova, O. Ersen, V. Valtchev, *Angew. Chem., Int. Ed.* **2016**, *55*, 15049.

[14] a) Y. Pan, G. Chen, G. Yang, X. Chen, J. Yu, *Inorg. Chem. Front.* **2019**, *6*, 1299; b) Y.-L. Zhu, H. Dai, Y. Duan, Q. Chen, M. Zhang, *Cryst. Growth Des.* **2020**, *20*, 2623.

[15] a) A. Buchholz, W. Wang, M. Xu, A. Arnold, M. Hunger, *Microporous Mesoporous Mater.* **2002**, *56*, 267; b) Z. Li, J. Martinez-Triguero, P. Concepcion, J. Yu, A. Corma, *Phys. Chem. Chem. Phys.* **2013**, *15*, 14670.

[16] a) D. Fan, P. Tian, X. Su, Y. Yuan, D. Wang, C. Wang, M. Yang, L. Wang, S. Xu, Z. Liu, *J. Mater. Chem. A* **2013**, *1*, 14206; b) G. Liu, P. Tian, Y. Zhang, J. Li, L. Xu, S. Meng, Z. Liu, *Microporous Mesoporous Mater.* **2008**, *114*, 416; c) Y. N. Huang, Z. M. Yan, R. Richer, *Chem. Mater.* **2005**, *17*, 6545; d) P. Tian, B. Li, S. T. Xu, X. Su, D. H. Wang, L. Zhang, D. Fan, Y. Qi, Z. M. Liu, *J. Phys. Chem. C* **2013**, *117*, 4048.

[17] H. J. Jung, C. H. Shin, S. B. Hong, *J. Phys. Chem. B* **2005**, *109*, 20847.

[18] a) L. Zhang, J. Bates, D. H. Chen, H. Y. Nie, Y. N. Huang, *J. Phys. Chem. C* **2011**, *115*, 22309; b) B. H. Chen, Y. N. Huang, *Microporous Mesoporous Mater.* **2009**, *123*, 71.

[19] Y. Qiao, M. Yang, B. Gao, L. Wang, P. Tian, S. Xu, Z. Liu, *Chem. Commun.* **2016**, *52*, 5718.

[20] H. Yang, Z. Liu, H. Gao, Z. Xie, *J. Mater. Chem.* **2010**, *20*, 3227.

Ji Han, Guoju Yang, Yongcun Zou, Xiaoxin Chen* and Valentin Valtchev

Hierarchical SAPO-34 preparation based on the crystal metastability in mother liquor solution

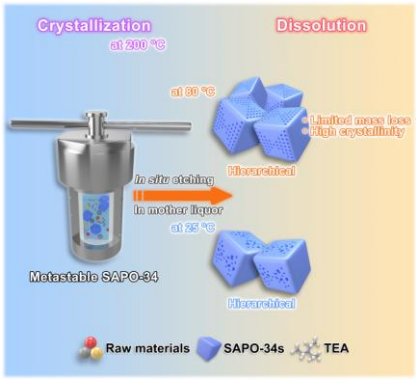

After the completion of zeolite crystallization, shifting the system to a lower temperature (25 to 80 °C) places the metastable zeolite in a non-equilibrium state, and thereby a partial dissolution process starts by *in situ* etching crystals. The hierarchical zeolites with high crystallinity and limited mass loss can be obtained conveniently via an extended hydrothermal treatment in the mother liquor without using any additional chemicals.